# Synthesis and Self-Assembly Behavior of Amphiphilic Polypeptide-Based Brush-Coil Block Copolymers

**CHUNHUA CAI, WENJIE ZHU, TAO CHEN, JIAPING LIN, XIAOHUI TIAN**

Shanghai Key Laboratory of Advanced Polymeric Materials, School of Materials Science and Engineering, East China University of Science and Technology, Shanghai 200237, China

*Received 21 May 2009; accepted 16 July 2009*
*DOI: 10.1002/pola.23640*
*Published online in Wiley InterScience (www.interscience.wiley.com).*

**ABSTRACT:** Synthesis and self-assembly behavior of a novel amphiphilic brush-coil block copolymer bearing hydrophilic poly(ethylene glycol) segment and hydrophobic polypeptide brush segment were presented in this work. The poly($\gamma$-benzyl-L-glutamate) (PBLG) brush is synthesized through "grafting from" strategy by ring-opening polymerization of $\gamma$-benzyl-L-glutamate-*N*-carboxyanhydride (BLG-NCA) initiated by the flanking terminal primary amino group of macroinitiator. The copolymers were characterized by $^1$H NMR, gel permeation chromatography, Fourier transform infrared, circular dichroism spectrum, and differential scanning calorimetry. The self-assembly behavior of the brush-coil block copolymers in aqueous solution was investigated by means of transmission electron microscopy, scanning electron microscopy, atomic force microscopy, and laser light scattering. Spherical micelles were observed when the length of PBLG brush is shorter. The aggregate morphology transforms to spindle-like micelles and then to rod-like micelles, as the length of polypeptide brush increases. © 2009 Wiley Periodicals, Inc. J Polym Sci Part A: Polym Chem 47: 5967–5978, 2009
**Keywords:** amphiphilics; brush copolymer; micelles; polypeptide; self-assembly

## INTRODUCTION

Polymeric micelles, self-assembled from amphiphilic block copolymers in selective solvents, have obtained much attention for their diversiform morphologies and promising potential applications.[1–6] With the progress of macromolecular chemistry, a variety of nonlinear copolymers including graft copolymers, star-like copolymers, and hyperbranched (dendrimer-like) copolymers have been synthesized, and these copolymers exhibit much more distinct self-assembly features when compared with linear block copolymers.[7–15] However, the understanding of the self-assembly behaviors of these nonlinear copolymers is not as deep as liner block copolymers.

Brush-like (comb-like) copolymers are a special class of graft copolymers, in which the side chains are distributed densely on a polymer backbone and the copolymers usually adopt an extended conformation in the high direction persistence.[16] In general, three main strategies have been successfully applied in synthesis of brush-like copolymers, including: "grafting from" (the polymerization of side chains from a macroinitiator backbone), "grafting onto" (the addition of previous prepared side chains to a backbone), and "grafting through" (the polymerization of macromonomers).[16]

In the past few years, both the unimolecular[17–19] and supramolecular micelles[20–26] from brush-like copolymers have been prepared. These brush-like copolymers show significant

*Correspondence to:* J. Lin (E-mail: jplinlab@online.sh.cn)
Journal of Polymer Science: Part A: Polymer Chemistry, Vol. 47, 5967–5978 (2009)

advantages in controlling the copolymer architecture, thus adjusting the self-assembly behaviors of the copolymers. Schmidt and coworkers have studied the synthesis and self-assembly behavior of poly{styrene-*block*-[(2-isobutyryloxy) ethyl methacrylate]-*graft*-(acrylic acid)} (PS-*b*-(PiBEMA-*g*-PAA)) brush-coil block copolymers.[20] The copolymers were observed to form star-like micelles in aqueous solution. Chen and coworkers synthesized amphiphilic comb-dendronized block copolymers composed of hydrophobic Percec-type dendronized polystyrene block and hydrophilic comb-like poly(ethylene oxide)-grafted polymethacrylate block via atom transfer radical polymerization.[21] By using such amphiphilic comb-dendronized block copolymers, rich morphologies, such as twisted string, vesicle, and large compound micelle, were obtained. Hadjichristidis and coworkers have studied the self-assembly behaviors of brush-like copolymers containing polystyrene, polyisoprene, or polybutadiene components with various architectures.[25] It was found that the macromolecular architecture affects the micellization behavior of the block copolymers. However, there is few work investigating the side brush length of hydrophobic blocks on the self-assembly behavior of the brush-like copolymers.

In many cases of the amphiphilic copolymers, poly(ethylene glycol) (PEG) segment is often used as the hydrophilic components because of its distinguished solubility in water, nonadhesive nature to proteins, and good biocompatibility.[27,28] Polypeptide, another biocompatible macromolecules, can serve as either hydrophilic or hydrophobic segments in amphiphilic copolymers.[29–37] Because of the inherent characters of PEG and polypeptide segments, copolymers based on these two components should be of substantial importance for the development of biomaterials, which are expected to play a key role in such fields as cell and tissue engineering, biosensing, and drug delivery systems.[38–41] Recently, our group has prepared polymeric micelles from both block and graft copolymers based on PEG and polypeptide segments, and a variety of structures such as spheres, spindles, rods, vesicles, and complex superhelices have been obtained.[42–45] In addition, the study on the drug loading and *in vitro* releasing behaviors shows that these polypeptide-based micelles may serve as a promising candidate in drug delivery system.[46–48]

In this work, we report the synthesis and self-assembly behavior of amphiphilic brush-coil block copolymers with PEG as hydrophilic segment and polypeptide as hydrophobic brush. The brush-like copolymers were synthesized by "grafting from" strategy using ring-opening polymerization (ROP) method. To our best knowledge, this is the first report on the synthesis and self-assembly behavior of brush-like copolymers with hydrophobic polypeptide brushes. The self-assembly behavior of the brush-coil block copolymers in aqueous solution was investigated. It was found that the length of polypeptide brush plays a key role in the morphology of the aggregates.

## EXPERIMENTAL

### Materials

Methoxypolyethylene glycol amine (PEG-$NH_2$, $M_w = 5000$) was purchased from Sigma and dissolved in toluene in a flame-dried reaction bottle, followed by removing toluene in high vacuum to obtain the sample used as initiator. Analytical grade of hexane, tetrahydrofuran (THF), and 1,4-dioxane were refluxed with sodium and distilled immediately before use. *N,N′*-dimethylformamide (DMF) was distilled under reduced pressure and stored over activated 4-Å molecular sieves. All other solvents are of analytical grade and used without further purification. γ-Benzyl-L-glutamate-*N*-carboxyanhydride (BLG-NCA) was synthesized according to the procedures reported in the literatures.[49,50] Dialysis bag (Membra-cel, 3500 molecular weight cutoff) was provided by Serva Electrophoresis GmbH.

### Synthesis

#### *Poly(ethylene glycol)*-block-*poly(γ-benzyl-L-glutamate)*

Poly(ethylene glycol)-*block*-poly(γ-benzyl-L-glutamate) (PEG-*b*-PBLG) block copolymer was synthesized by ROP of BLG-NCA, initiated by the terminal primary amino groups of PEG-$NH_2$.[49–54] Briefly, PEG-$NH_2$ (0.25 g, 0.05 mmol) and BLG-NCA (1.8 g, 6.8 mmol) were dissolved in dioxane separately in two flame-dried reaction bottles, and then BLG-NCA solution was added to the solution of PEG-$NH_2$ via a transfer cannula. The final concentration of BLG-NCA was about 2 wt %. The reaction was performed at 15 °C under a dry nitrogen atmosphere. After 72-h stirring, the reaction mixture became a viscous liquid and was poured into a large volume of anhydrous

ethanol. The precipitated products were collected by filter and dried under vacuum. The products were purified twice by repeated cycles of dissolution in chloroform and precipitation in anhydrous methanol. Finally, 1.3 g of white powder was obtained.

### *Poly(ethylene glycol)*-block-*poly((2-aminoethyl)-L-glutamate)*

Poly(ethylene glycol)-*block*-poly((2-aminoethyl)-L-glutamate) (PEG-*b*-P(ELG-$NH_2$)) macroinitiator was prepared from PEG-*b*-PBLG by aminolysis of flanking benzyl ester groups with 1,2-diaminoethane (DAE) as described in literature.[51] Briefly, 1 g of PEG-*b*-PBLG block copolymer (contains 3.8 mmol benzyl groups) was dissolved in 40 mL of dry DMF. A total of 13 mL DAE (11.5 g, 190 mmol, 50 eq relative to benzyl groups of PBLG) was then added and the mixture solution was stirred at 40 °C under a nitrogen atmosphere. After 24 h, 80 mL of 10 vol % acetic acid was added and stirred for 5 h at 0 °C. The reaction mixture was dialyzed against deionized water for 3 days at room temperature and freeze-dried to get the final product (0.5 g).

### *Poly(ethylene glycol)*-block-*poly(((2-aminoethyl)-L-glutamate)*-graft-*poly(γ-benzyl-L-glutamate))*

Poly(ethylene glycol)-*block*-poly(((2-aminoethyl)-L-glutamate)-*graft*-poly(γ-benzyl-L-glutamate)) (PEG-*b*-P(ELG-*g*-PBLG)) brush-coil block copolymers were synthesized through "grafting from" strategy by ROP of BLG-NCA initiated by the flanking terminal primary amino group of PEG-*b*-P(ELG-$NH_2$) macroinitiator. The reaction conditions and products purification methods are all similar to the synthesis of PEG-*b*-PBLG block copolymer as described earlier. Taking PEG-*b*-P(ELG-*g*-PBLG)-1, for example, PEG-*b*-P(ELG-$NH_2$) (40 mg, 0.19 mmol of flanking primary amino residues) and BLG-NCA (1.7 g, 0.64 mmol) were dissolved in dioxane separately in two reaction bottles and then mixed together via a transfer cannula. After purification and drying, 1.2 g of PEG-*b*-P(ELG-*g*-PBLG)-1 brush-coil block copolymer was obtained. By the variation of molar ratio of PEG-*b*-P(ELG-$NH_2$) macroinitiator to BLG-NCA, the degree of the polymerization of PBLG brush could be adjusted. Finally, four brush-coil block copolymers, denoted as PEG-*b*-P(ELG-*g*-PBLG)-1, 2, 3, and 4, were obtained.

### *Preparation of Micelles*

The polymeric micelle solutions were prepared using a dialysis method. The brush-coil block copolymer (3 mg) was first dissolved in 10 mL of a mixed solvent of THF/DMF (3/7, v/v) and stored overnight at room temperature. Then, deionized water (2.5 mL), a selective solvent for PEG segment, was added at a rate of one drop (ca. 0.02 mL) per second with vigorous stirring. Next, the solution was stabilized under stirring for at least 6 h. Finally, the solution was dialyzed against deionized water for 3 days at room temperature. Before analysis, the micelle solutions were stabilized for at least 5 days.

## Measurements

### *$^1$H NMR*

The degree of polymerizations (DPs) of PBLG segments, both in PEG-*b*-PBLG block copolymer and PEG-*b*-P(ELG-*g*-PBLG) brush-coil block copolymers, were estimated using $^1$H NMR measurements. $^1$H NMR spectra measurements were performed on a Bruker Avance 550 spectrometer using deuterated chloroform ($CDCl_3$) as solvent and tetramethylsilane as an internal standard at room temperature. The structure of PEG-*b*-P(ELG-$NH_2$) macroinitiator was detected by $^1$H NMR spectrum using deuterium oxide ($D_2O$) as solvent.

### *Gel Permeation Chromatography*

The polydispersity indices (PDIs) of original PEG-*b*-PBLG block copolymer and PEG-*b*-P(ELG-*g*-PBLG) brush-coil block copolymers were determined by GPC (Waters 1515 instrument) with DMF as mobile phase at room temperature.

### *Fourier Transform Infrared Spectrum*

FTIR spectra of the copolymers were recorded on a Nicolet 5700 FTIR spectrometer at frequencies ranging from 400 to 4000 $cm^{-1}$. The solid samples were thoroughly mixed with KBr and pressed into pellet form. The tests were performed at room temperature.

### *Circular Dichroism*

CD analyses of the polypeptides were performed with a JASCO J810 spectrometer at room temperature. The solvents are water for PEG-*b*-P(ELG-$NH_2$) and THF for PEG-*b*-P(ELG-*g*-PBLG)

copolymers, respectively. The diluted solutions (0.075 g $L^{-1}$ for all the samples) were introduced in quartz cells with 1 cm optical path length. Wavelengths between 200 and 300 nm were analyzed, with an integration time of 1 s and a wavelength step of 0.2 nm. The molar ellipticity $[\theta]$ of the polymers can be calculated according to the following equation: $[\theta] = \theta/(10\ ML)$, where $\theta$, $M$, and $L$ are the absorption value of polymer solutions (mdeg), molar concentration of the peptide units (mol $L^{-1}$), and optical path length of quartz cell (cm), respectively. In addition, from value of $[\theta]$, the helix content of the polypeptides can be estimated (helix content [%] = $([\theta]/[\theta]_h)\times 100\%$, where $[\theta]_h$ is $-34{,}000$ deg $cm^2$ $dmol^{-1}$).[55]

### Differential Scanning Calorimetry

DSC experiments were carried out on a Diamond DSC differential scanning spectrometer (Perkin–Elmer) at a heating rate of 10 °C/min over a temperature range from −50 to 150 °C under a nitrogen atmosphere.

### Transmission Electron Microscopy

The morphologies of the aggregates were examined by TEM (JEOL/JEM-2000EXII) operated at an accelerating voltage of 60 kV. Drops of micelle solution were placed on a copper grid coated with carbon film and then were dried at room temperature. Before the observations, the sample was stained by phosphotungstic acid aqueous solution (0.5 wt %).

### Scanning Electron Microscopy

The surface profile of the aggregates was obtained from SEM (JSM-6460, JEOL) operated at an accelerating voltage of 20 kV. The sample was prepared by placing drops of solution on a copper grid coated with carbon film and then were dried at room temperature. Before the observations, the samples were sputtered by carbon.

### Atomic Force Microscopy

AFM image was obtained with a multimode atomic force microscopy (Veeco/Nanoscope IIIa), using the tapping mode. The sample was prepared by placing a drop of solution on a fresh-cleaved mica surface and allowed to dry in air.

### Light Scattering Measurements

Laser light scattering was measured by a LLS spectrometer (ALV/CGS-5022) equipped with an ALV-High QE APD detector and an ALV-5000 digital correlator using a He–Ne laser (the wavelength $\lambda = 632.8$ nm) as the light source. All the measurements were carried out at 20 °C. In static LLS, the angular dependence of the excess absolute time-average scattered intensity, that is, Rayleigh ratio $R_{vv}(q)$ of the dilute dispersion leads to the root-mean-square $z$-average radius of gyration $\langle R_g \rangle$, where $q = 4\pi n \sin(\varphi/2)/\lambda$ is the scattering vector as a function of scattering angle $\varphi$, $n$ is the refractive index of the solution, and $\lambda$ is the wavelength of the incident bean. In dynamic LLS measurement, the Laplace inversion of each measured intensity–intensity time correlation function $G^{(2)}(t, q)$ in the self-beating mode can result in a line width distribution $G(\Gamma)$. The translational diffusion coefficient $D$ calculated from the decay time, $\Gamma$, by the slope of the $\Gamma$ versus $q^2$ plot can lead to hydrodynamic radius $R_h$ by the Stokes–Einstein equation $R_h = k_B T/(6\pi\eta D)$, where $k_B$, $T$, and $\eta$ are the Boltzmann constant, the absolute temperature, and the solvent viscosity, respectively.

## RESULTS AND DISCUSSION

### Synthesis and Characterization of the Block and Brush-Coil Copolymers

The synthesis of amphiphilic polypeptide-based brush-coil block copolymers, PEG-*b*-P(ELG-*g*-PBLG), was achieved by three consecutive steps as illustrated in Scheme 1 in detail.

First, PEG-*b*-PBLG block copolymer was prepared by ROP of BLG-NCA initiated by the terminal primary amino groups of PEG-$NH_2$. Next, by aminolysis reaction with DAE, the flanking benzyl ester unit of PBLG block was converted into a primary amino group, which was further used to initiate the polymerization of BLG-NCA. Because of the large excess amount of DAE to benzyl ester group and strong steric effect of huge PBLG chains, the side reactions including intra- and intermolecular crosslink reaction could be avoided or minimized. Finally, PEG-*b*-P(ELG-*g*-PBLG) brush-coil block copolymers were prepared by "grafting from" strategy. The PBLG brushes were synthesized by ROP of BLG-NCA initiated by the flanking primary amino groups of PEG-*b*-P(ELG-$NH_2$) macroinitiator. The length of PBLG brush was controlled by adjusting the feeding molar

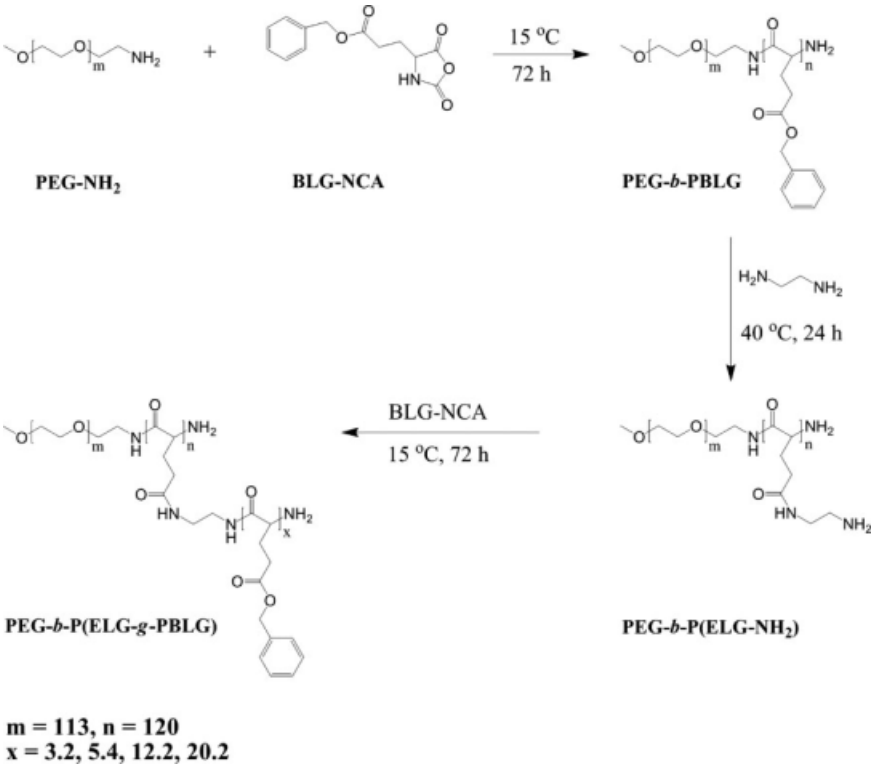


**Scheme 1.** Synthetic route of the polypeptide-based brush-coil block copolymers.

amount of BLG-NCA to macroinitiator. It should be noted that the amino end group on PEG-*b*-P(ELG-$NH_2$) backbone may also initiate the ROP of BLG-NCA, which could lead to a linear extension of the polypeptide backbone. However, because there is a large amount of active amino groups on the side chains, the linear extension polymerization of the polypeptide backbone should be not obvious. Therefore, as an acceptable simplification, only "grafting from" process of PBLG brush was considered.

The schematic representation of PEG-*b*-P(ELG-*g*-PBLG) brush-coil block copolymer is shown in Scheme 2. The copolymer consists of a hydrophilic flexible PEG block and a hydrophobic brush-like polypeptide block in which both the backbone and the brush are derived from polypeptides. As it is highly grafted with PBLG brushes, the polypeptide backbone could be highly extended.

The molecular composition of PEG-*b*-PBLG block copolymer was estimated by $^1$H NMR measurement, as shown in Figure 1(a). As the molecular weight of PEG block is known (5000, DP = 113), the molecular weight of PBLG block of PEG-*b*-PBLG block copolymer can be calculated by the peak intensities of the methylene proton signal (5.1 ppm) of PBLG and the ethylene proton signal (3.6 ppm) of PEG in the $^1$H NMR spectrum.[45,51] According to the $^1$H NMR analysis, the molecular weights of PBLG block and total block copolymer are calculated to be 26,300 and 31,300, respectively. The $^1$H NMR spectrum of PEG-*b*-P(ELG-$NH_2$) macroinitiator in $D_2O$ [Fig. 1(b)] shows that the benzyl groups were completely replaced by DAE, indicated by the disappearance of methylene (5.1 ppm) and benzyl proton peak

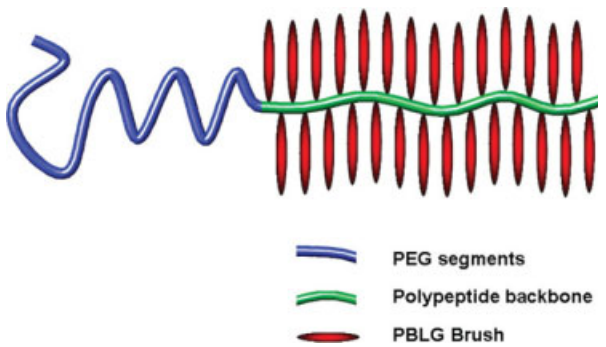


**Scheme 2.** Schematic representation of PEG-*b*-P(ELG-*g*-PBLG) brush-coil block copolymer. The blue, green, and red lines are assigned to indicate the PEG blocks, polypeptide backbones, and PBLG brushes, respectively.

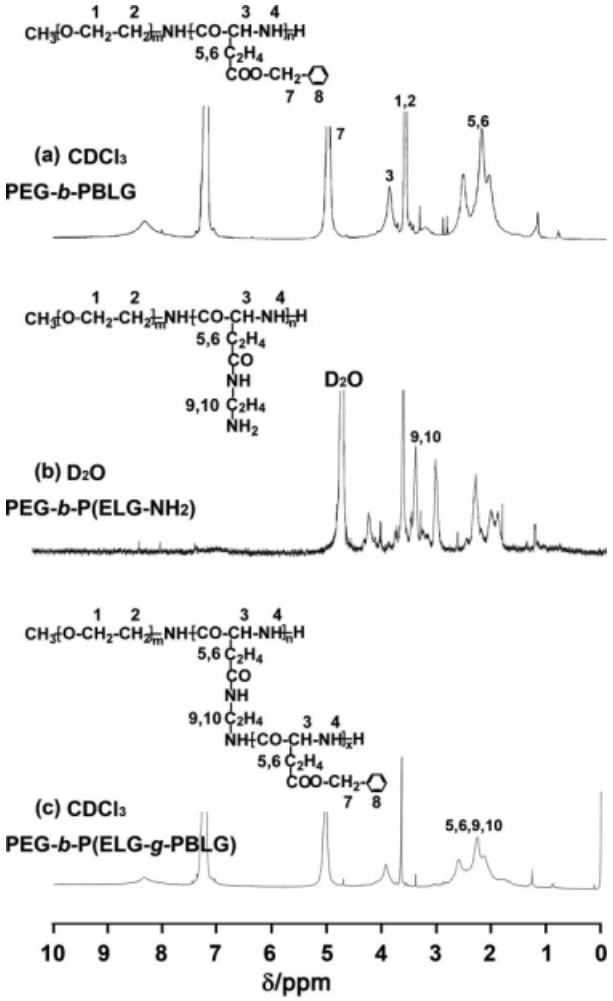


**Figure 1.** $^1$H NMR spectra of (a) PEG-*b*-PBLG block copolymer, (b) PEG-*b*-P(ELG-$NH_2$) macroinitiator, and (c) PEG-*b*-P(ELG-*g*-PBLG)-4 brush-coil block copolymer.

(7.27 ppm) of PBLG segments and the appearance of ethylene proton signals (3.2–3.4 ppm) from DAE side chains. Shown in Figure 1(c) is a typical $^1$H NMR spectrum of PEG-*b*-P(ELG-*g*-PBLG)-4 in $CDCl_3$, the presence of benzyl proton peak (7.27 ppm) of PBLG segments indicates the formation of brush-coil block copolymers. According to the peak intensities of the methylene proton signal (5.1 ppm) of PBLG and the ethylene proton signal (3.6 ppm) of PEG, the DP of PBLG brushes and the total molecular weights of the PEG-*b*-P(ELG-*g*-PBLG) brush-coil block copolymers can be calculated. As listed in Table 1, with increasing the length of PBLG brush, the molecular weight of the copolymer increases sharply, and the weight fraction of EG unit decreases markedly.

Figure 2 shows the GPC traces of the original PEG-*b*-PBLG block copolymer and PEG-*b*-P(ELG-*g*-PBLG) brush-coil block copolymers. All the samples showed a monomodal symmetric distribution, indicating a well-controlled polymerization process and a success on the synthesis of copolymers. Comparing with the low PDI (1.2) of original PEG-*b*-PBLG block copolymer, the PDIs of the brush-coil block copolymers were broadening to 1.6–2.0. Detailed information regarding the characteristics of original PEG-*b*-PBLG block copolymer and PEG-*b*-P(ELG-*g*-PBLG) brush-coil block copolymers is provided in Table 1.

The polymers were also characterized by FTIR measurement (Fig. 3). The IR spectrum of PEG-*b*-PBLG block copolymer [Fig. 3(a)] displayed two bands at 1652 and 1547 $cm^{-1}$, suggesting that the amide I and II bands of PBLG backbone adopt the α-helix conformation.[37,56,57] The bands at 1734 and 1167 $cm^{-1}$ indicate the presence of ester groups of PBLG. The bands appearing at 747 and

**Table 1.** Characteristics of PEG-*b*-P(ELG-*g*-PBLG) Brush Copolymers

| Entry | $x$[a] | $M_n$[b] | PDI[c] | EG wt %[d] |
|---|---|---|---|---|
| PEG-*b*-PBLG | 0 | 31,300 | 1.23 | 16.1 |
| PEG-*b*-P(ELG-*g*-PBLG)-1 | 3.2 | 110,000 | 2.01 | 4.5 |
| PEG-*b*-P(ELG-*g*-PBLG)-2 | 5.4 | 167,000 | 1.61 | 3.0 |
| PEG-*b*-P(ELG-*g*-PBLG)-3 | 12.6 | 357,000 | 2.01 | 1.4 |
| PEG-*b*-P(ELG-*g*-PBLG)-4 | 20.2 | 556,000 | 2.02 | 0.9 |

[a] $x$ is the degree of polymerization of the flanking PBLG brush of PEG-*b*-P(ELG-*g*-PBLG) copolymers, and it is derived from $^1$H NMR spectrum. For PEG-*b*-PBLG original block copolymer, $x = 0$.
[b] Number-average molecular weights ($M_n$) of copolymers are calculated according to the $^1$H NMR spectra.
[c] Polydispersity indices (PDIs) of the copolymers are determined by GPC.
[d] EG wt % is the weight fraction of PEG segments in the copolymers.

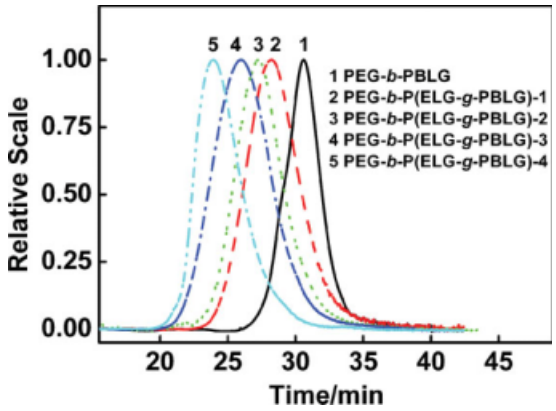


**Figure 2.** GPC traces of PEG-*b*-PBLG block copolymer and PEG-*b*-P(ELG-*g*-PBLG) brush-coil block copolymers. [Color figure can be viewed in the online issue, which is available at www.interscience.wiley.com.]

696 $cm^{-1}$ are characteristic vibration of benzyl groups. The peak at 3294 $cm^{-1}$ is assigned to N—H vibration of PBLG backbone. The ether groups of PEG segment show two characteristic peaks at 1120 and 967 $cm^{-1}$. The FTIR spectrum indicates that PEG-*b*-PBLG block copolymer was successfully synthesized. For PEG-*b*-P(ELG-$NH_2$) copolymer, as shown in Figure 3(b), both the bands of benzyl groups (747 and 696 $cm^{-1}$) and ester groups (1734 and 1167 $cm^{-1}$) vanish because the benzyl ester groups were replaced completely by DAE as indicated by $^1H$ NMR spectrum [Fig. 1(b)]. However, the band of N—H vibration (3294 $cm^{-1}$) becomes much more obvious when compared with Figure 3(a), which is induced by the introduction of a large amount of N—H groups from DAE. Figure 3(c,d) gives the FTIR spectra of PEG-*b*-P(ELG-*g*-PBLG)-1 and 4 copolymers, respectively. The spectra give very similar results with that of PEG-*b*-PBLG block copolymer, indicating the introduction of PBLG segments. Additionally, FTIR spectra also provide conformation information of polypeptide segments. As shown in Figure 3(a), in the amide II band region, there is a sharp peak at 1547 $cm^{-1}$, which suggests an α-helix structure of PBLG segments in PEG-*b*-PBLG block copolymer. For PEG-*b*-P(ELG-$NH_2$), the amide II band is very broad and slightly red-shifted [Fig. 3(b)], suggesting that the polypeptide backbone mainly takes random coil conformation.[56] For PEG-*b*-P(ELG-*g*-PBLG) brush-coil copolymers, when the DP of PBLG brush is low, as shown in Figure 3(c) for PEG-*b*-P(ELG-*g*-PBLG)-1, the broad amide II band indicates that the polypeptide segments mainly take random coil conformation, as well as minor α-helix conformation which is attributed to the PBLG brushes. For PEG-*b*-P(ELG-*g*-PBLG)-4, there is a sharp peak in the amide II band region, which suggests an α-helix structure of PBLG brushes.

The secondary structure of the polypeptide segments was further characterized by CD, as shown in Figure 4. The CD spectra show that the polypeptide segments of PEG-*b*-P(ELG-$NH_2$) block copolymer take random coil conformation in neutral aqueous solution. This is in agreement with the fact that water-soluble poly(amino acid)s usually take random coil conformation.[29,30,44,58] The random coil chain could be extended when PBLG brush is grafted on, because of the strong steric repulsion between PBLG brushes. For PEG-*b*-P(ELG-*g*-PBLG) brush-coil block copolymers, the spectra show a negative minimum around 228 nm, indicating that the PBLG brush adopts α-helix conformation.[43,44] The calculations show that the α-helix content of PBLG brush gradually increases from <10% to about 80%, when the DP of PBLG brush increases from 3 to 20. It was reported that PBLG with DP less than 4 cannot form α-helix conformation; when the DP is larger than 10, stable α-helix conformation can be formed.[59] However, for this system, because of the broad PDIs of the brush-coil block copolymers, there exist some PBLG brushes with relative higher DP, thus PEG-*b*-P(ELG-*g*-PBLG)-1 copolymers show α-helix characteristic absorption in CD spectrum (Fig. 4, curve 2). These CD results for the second structure of polypeptide segments are in good agreement with FTIR testing.

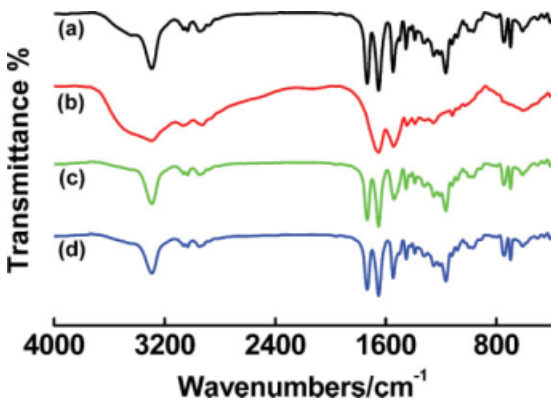


**Figure 3.** FTIR spectra of (a) PEG-*b*-PBLG, (b) PEG-*b*-P(ELG-$NH_2$), (c) PEG-*b*-P(ELG-*g*-PBLG)-1, and (d) PEG-*b*-P(ELG-*g*-PBLG)-4 copolymers. [Color figure can be viewed in the online issue, which is available at www.interscience.wiley.com.]

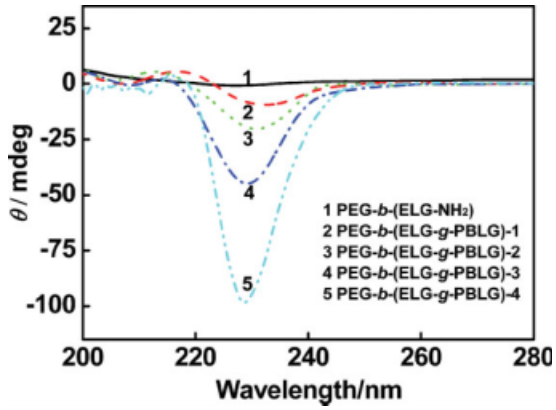


**Figure 4.** CD spectra of PEG-*b*-P(ELG-$NH_2$) block copolymer in water and PEG-*b*-P(ELG-*g*-PBLG) brush-coil block copolymers in THF. [Color figure can be viewed in the online issue, which is available at www.interscience.wiley.com.]

The thermal behaviors of these copolymers were investigated with DSC measurements carried out from −50 to 150 °C (Fig. 5). As shown in Figure 5(a), the thermogram of the PEG-*b*-PBLG block copolymer shows three transitions: the first (−25 °C) is the glass transition of PEG segment, the second (17 °C) is the glass transition of PBLG segment,[57] and the third (60 °C) is the melting transition of PEG segment. For PEG-*b*-P(ELG-$NH_2$), the glass transition of PBLG segment vanished, but a new transition around 95 °C appeared [Fig. 5(b)], which corresponds to the melting transition of P(ELG-$NH_2$) segment. Shown in Figure 5(c,d) are the DSC curves of PEG-*b*-P(ELG-*g*-PBLG)-1 and 4, respectively, which show the glass transition of PEG segment (−25 °C), the glass transition of PBLG segment (17 °C), and the melting transition of PEG segment (60 °C), respectively.

## Self-Assembly Behavior of Brush-Coil Copolymers in Water

PEG-*b*-P(ELG-*g*-PBLG) brush-coil block copolymers presented herein are highly asymmetric, that is, they bear low weight fraction of PEG segments (ranging from 0.9 to 4.5 wt %, see Table 1). It is well know that, for asymmetric copolymers, dialysis method is an effective way to prepare polymeric micelles. To produce uniform self-assembled aggregates, premicellization process by adding selective solvent before dialysis is necessary. Eisenberg's group has done much on the micellization of highly asymmetric block copolymers, such as polystyrene-*b*-poly(acrylic acid) and polystyrene-*b*-poly(ethylene oxide).[3,4] It was found that the stable aggregates can be produced even when the weight fraction of hydrophilic poly (acrylic acid) (PAA) segment is lower to about 1%. Because of its extreme good solubility, PEG-based amphiphilic copolymers bearing very low PEG fraction can self-assemble into polymeric micelles in aqueous solution.[27,28] For this system, PEG-*b*-P(ELG-*g*-PBLG) brush-coil block copolymer dissolves well in THF/DMF mixed solvent, when water, a strong selective solvent for PEG segment was dropped into, the solubility of mixed solvent (THF/DMF/$H_2O$) for PEG blocks still remains well, but becomes worse for polypeptide segments. With gradually increasing of water content, hydrophobic polypeptide segments become insoluble and tend to aggregate to form micelle core outspreaded with soluble PEG chains.[3,4] Finally, through dialysis process, stable polymeric micelle aqueous solutions were obtained. The aggregate morphologies and structures were tested by TEM, SEM, AFM, and LLS.

## Morphologies of the Brush-Coil Copolymer Aggregates

Figure 6 displays TEM photographs of aggregate formed by PEG-*b*-P(ELG-*g*-PBLG) brush-coil block copolymers. The brush-coil block copolymer with shortest brush length (PEG-*b*-P(ELG-*g*-PBLG)-1) forms spherical micelles with a diameter of about 80 nm, as shown in Figure 6(a). As the length of PBLG brush increases, the aggregate morphology transforms to spindle-like micelles [Fig. 6(b), PEG-*b*-P(ELG-*g*-PBLG)-2]

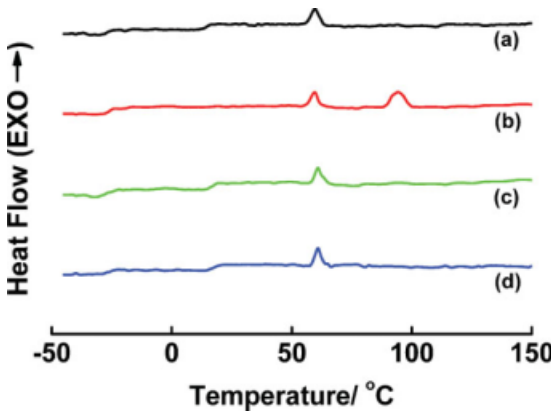


**Figure 5.** DSC curves of (a) PEG-*b*-PBLG, (b) PEG-*b*-P(ELG-$NH_2$), (c) PEG-*b*-P(ELG-*g*-PBLG)-1, and (d) PEG-*b*-P(ELG-*g*-PBLG)-4 copolymers. [Color figure can be viewed in the online issue, which is available at www.interscience.wiley.com.]

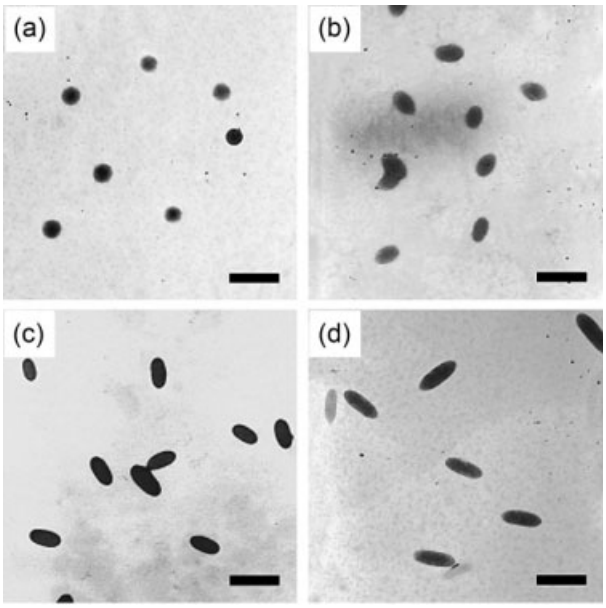


**Figure 6.** TEM images of PEG-*b*-P(ELG-*g*-PBLG) aggregates self-assembled in aqueous solution: (a) PEG-*b*-P(ELG-*g*-PBLG)-1, (b) PEG-*b*-P(ELG-*g*-PBLG)-2, (c) PEG-*b*-P(ELG-*g*-PBLG)-3, and (d) PEG-*b*-P(ELG-*g*-PBLG)-4. The scale bars represent 200 nm.

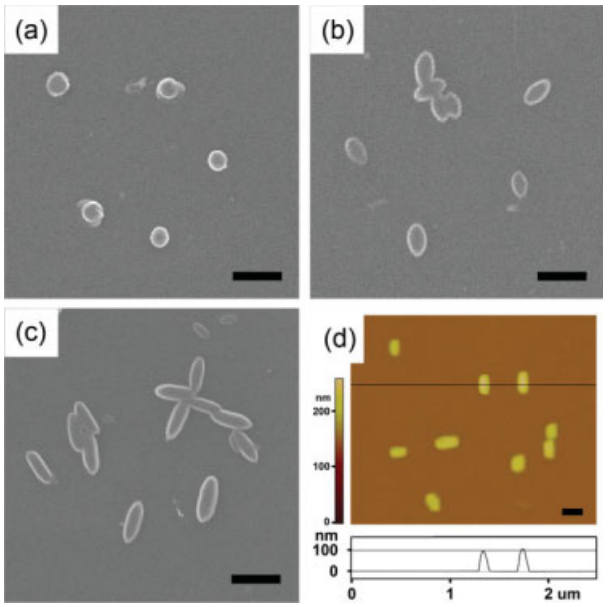


**Figure 7.** SEM images of aggregates self-assembled from PEG-*b*-P(ELG-*g*-PBLG)-1 (a), PEG-*b*-P(ELG-*g*-PBLG)-2 (b), and PEG-*b*-P(ELG-*g*-PBLG)-4 (c); and AFM image of rod-like micelle self-assembled from PEG-*b*-P(ELG-*g*-PBLG)-4 (d). The scale bars represent 200 nm. [Color figure can be viewed in the online issue, which is available at www.interscience.wiley.com.]

and then to rod-like micelles [Fig. 6(c,d), PEG-*b*-P(ELG-*g*-PBLG)-3 and 4, respectively]. The diameter of the spindles and rods keeps about 90 nm. The spindle looks like a one-dimensional elongated sphere, its width decreases linearly from the middle to the ends; however, for the rod-like micelle, it has a constant width on the main body. And, the length–diameter ($L/D$) ratio of rods is much larger than spindles.

The morphologies of these aggregates are also provided by the SEM and AFM observations (Fig. 7). Shown in Figure 7(a–c) are the typical SEM images of spherical micelles, spindle-like micelles, and rod-like micelles self-assembled from PEG-*b*-P(ELG-*g*-PBLG)-1, 2, and 4, respectively. The SEM images clearly give three-dimensional shapes of the aggregates. The AFM image for rod-like micelles self-assembled from PEG-*b*-P(ELG-*g*-PBLG)-4 is represented in Figure 7(d). The cross-section profile of the aggregates shows that the height and the width are similar in size, which proves the three-dimensional rod-like structure of the self-assembled aggregates. Both SEM and AFM analysis of the aggregates are in line with the TEM results.

### Aggregate Size and Structure Studied by LLS

The aggregate structures of PEG-*b*-P(ELG-*g*-PBLG) brush-coil block copolymers were further studied by LLS. Figure 8 shows that both the average hydrodynamic radius ($\langle R_h \rangle$) and average radius of gyration ($\langle R_g \rangle$) of the aggregates increase markedly with increasing the DP of PBLG brush from 3 to 20. As can be seen in Figure 8, the $\langle R_g \rangle$ increases more sharply than $\langle R_h \rangle$ does. This is because they are defined in different ways, namely, $\langle R_h \rangle$ is the radius of a hard sphere with

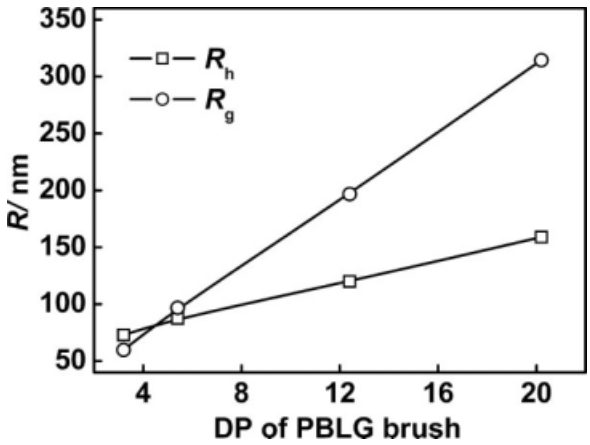


**Figure 8.** Plots of $\langle R_h \rangle$ and $\langle R_g \rangle$ value of the aggregates as a function of PBLG brush length.

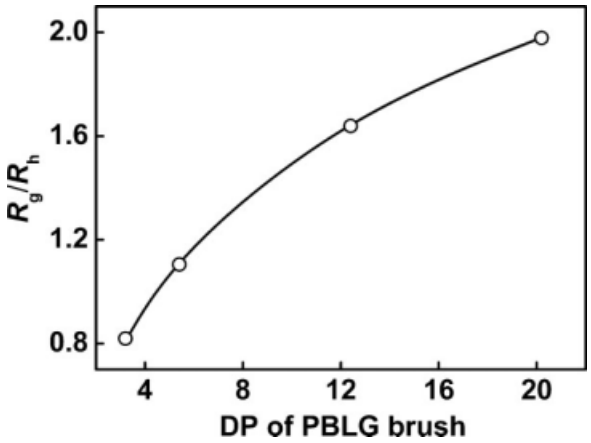


**Figure 9.** Plots of $\langle R_g \rangle / \langle R_h \rangle$ value of the aggregates as a function of PBLG brush length.

the same translational diffusion coefficient and the same condition, whereas $\langle R_g \rangle$ reflects the density distribution of the chain in real physical space.[60] The sharp increase of $\langle R_g \rangle$ can be contributed to the morphology changes from spheres to rods, which has also been observed by TEM and SEM testing.

The micelle shape can be also viewed in terms of the ratio of $\langle R_g \rangle / \langle R_h \rangle$, which is sensitive to the particle shape.[60,61] Generally, $\langle R_g \rangle / \langle R_h \rangle = 0.774$ is thought as a uniform and nondraining sphere; and for a rigid rod structure, the ratio $\langle R_g \rangle / \langle R_h \rangle$ should be a large value. As shown in Figure 9, with the DP of PBLG brush increased from 3 to 20, the $\langle R_g \rangle / \langle R_h \rangle$ value increases from 0.82 to 1.98, which corresponds to the micelle morphology transformation from spheres to spindles and then to rods.

Based on the experimental results, the mechanism of the micelle structure transition of brush-coil block copolymers was proposed (as illustrated in Scheme 3). For PEG-*b*-P(ELG-*g*-PBLG) brush-coil block copolymers with short PBLG brush, the mass fraction of hydrophilic PEG segment is relative higher, it prefers to self-assemble into spherical micelles with hydrophobic brush blocks form micelle core and hydrophilic PEG chains outspread to stabilize the aggregates, as illustrated in Scheme 3(a). With increasing the DP of PBLG brush, the excluding volume of the brush blocks increases, and the mass fraction of hydrophilic PEG segment decreases. As a result, the distance between the PEG chains in the micelle shell increases, and thus the repulsion force among the corona chains decreases. To make PEG chains can shield the hydrophobic polypeptide blocks from exposing to the water effectively, the aggregates morphology prefer to transform to those with lower interfacial curvature.[1,2,62,63] Resultantly, the aggregate morphology transformed to rod-like micelles [Scheme 3(c)]. Besides spheres and rods, the brush-coil block copolymers with moderate length of PBLG brush form spindle-like micelles, as illustrated in [Scheme 3(b)]. The spindle is not a common morphology observed from self-assembly systems,[42,64] and it looks like an elongated sphere. As shown in Scheme 3, the molecular aggregations in sphere, spindle, and rod are different, and the interfacial curvature of spindles is lower than spheres but larger than rods.

As indicated by the previous work, with the decrease of the weight fraction of hydrophilic blocks, the aggregate morphology was observed to transform to those with lower interfacial curvature, that is, from spheres to cylinders and then to vesicles.[1–4] In this case, the key contribution for the morphology transition is the hydrophilic corona chain repulsion, as the block length ratio of hydrophilic–hydrophobic segments was varied.[62] A polymer chain can be viewed as a three-dimensional cylinder structure, there is two effective way to increase the volume of the polymer chain, that is, increasing its length or diameter. Increasing the length of block chain is a common way to alter the weight ratio of hydrophilic–hydrophobic segments of simple linear block copolymers. In this work, we present a different approach to adjust the weight fraction of hydrophilic blocks by changing the diameter of the hydrophobic block cylinder, as the result of the variation of the length of flanking brush

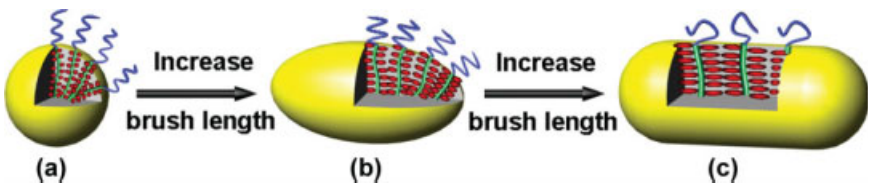


**Scheme 3.** Schematic representation of the morphology transition from spheres (a) to spindles (b) and then to rods (c), as the PBLG brush length increases. [Color figure can be viewed in the online issue, which is available at www.interscience.wiley.com.]

segments. The increase of the diameter of hydrophobic polypeptide block cylinder increases the distance between hydrophilic PEG segments in the aggregate corona region, which decreases the repulsion between PEG blocks; as a result, the aggregate morphology was observed to transform from spheres to spindles and then to rods. On the other hand, when compared with the linear extension of the hydrophobic block cylinder, increasing its diameter makes the hydrophilic segments stabilize the aggregates much easily. Although the weight fraction of hydrophobic segment increases markedly, the aggregates can maintain a relative small size.

Additionally, from the TEM, SEM, and AFM images shown in Figures 6 and 7, we find that the diameter of the aggregates keeps almost the same value (ca. 80–90 nm), which indicates that these aggregates have a similar intermolecular packing mode. As stated earlier, the polypeptide backbone takes extended coil conformation in solution, thus the brush-coil block copolymers act similarly with rod-coil type block copolymers. The rod-like hydrophobic brush blocks prefer to take ordered packing mode during aggregation,[65–67] as schematically illustrated in Scheme 3. It is widely reported that the per unit length of polypeptide backbone is 0.37 nm when fully stretched.[29–32,43] Therefore, the length of the polypeptide backbone of the brush block can be estimated. From the polymerization degree of polypeptide backbone (120), the theoretical arithmetic value of the hydrophobic segments length is estimated to be about 30–40 nm, close to the radius of the micelle as revealed in microscopic images (Figs. 6 and 7). On considering the large volume of PBLG brushes, the stretch content should increase with increasing the PBLG brush length, which explains the slightly smaller diameter of spheres comparing with spindles and rods. It should be noted that the aggregate size from the microscopy observations also includes the PEG coronas though they are mostly collapsed during the preparation of the samples for the microscopy observations. In this view, the proposed mechanism for the aggregate structures and the structure transition illustrated in Scheme 3 is reasonable.

## CONCLUSIONS

In summary, a novel of amphiphilic polypeptide-based brush-coil block copolymer with various brush length was synthesized and characterized with NMR, GPC, IR, CD, and DSC. The self-assembly behavior of these brush copolymers in aqueous solution was investigated by TEM, SEM, AFM, and LLS. It revealed that with increasing of the length of polypeptide brush, the aggregate morphology transform from spheres to spindles and then to rods. Summarizing the experimental results, the mechanism of the structure change of the aggregates self-assembled from brush-like copolymers was suggested. The brush copolymers and the formed self-assemblies can be easily functionalized because there are a large amount of high-reactive amino groups at the end of the polypeptide brushes, which can facilitate the application of these polypeptide-based brush copolymers and self-assembled aggregates as bio-related materials, for example, drug delivery systems.

This work was supported by National Natural Science Foundation of China (50673026). Supports from Projects of Shanghai Municipality (09XD1401400, 082231, 0952nm05100, B502, and 08DZ2230500) are also appreciated.

## REFERENCES AND NOTES

1. Jain, S.; Bates, F. S. Science 2003, 300, 460–464.
2. Riess, G. Prog Polym Sci 2003, 28, 1107–1170.
3. Zhang, L.; Eisenberg, A. Polym Adv Technol 1998, 9, 677–699.
4. Zhang, L.; Eisenberg, A. J Am Chem Soc 1996, 118, 3168–3181.
5. Dalhaimer, P.; Engler, A. J.; Parthasarathy, R.; Discher, D. E. Biomacromolecules 2004, 5, 1714–1719.
6. Rosler, A.; Vandermeulen, G. W. M.; Klok, H. A. Adv Drug Delivery Rev 2001, 53, 95–108.
7. Hadjichristidis, N.; Iatrou, H.; Pitsikalis, M.; Mays, J. Prog Polym Sci 2006, 31, 1068–1132.
8. Peleshanko, S.; Tsukruk, V. V. Prog Polym Sci 2008, 33, 523–580.
9. Lee, H. J.; Yang, S. R.; An, E. J.; Kim, J.-D. Macromolecules 2006, 39, 4938–4940.
10. Wang, C.; Li, G.; Guo, R. Chem Commun 2005, 3591–3593.
11. Li, Z.; Hillmyer, M. A.; Lodge, T. P. Macromolecules 2006, 39, 765–771.
12. Zhang, Y.; Liu, H.; Dong, F.; Li, C.; Liu, S. J Polym Sci Part A: Polym Chem 2009, 47, 1636–1650.
13. Pispas, S.; Hadjichristidis, N.; Potemkin, I.; Khokhlov, A. Macromolecules 2000, 33, 1741–1746.
14. Bosman, A. W.; Janssen, H. M.; Meijer, E. W. Chem Rev 1999, 99, 1665–1688.
15. Zhou, Y.; Yan, D. Angew Chem Int Ed 2004, 43, 4896–4899.
16. Sheiko, S. S.; Sumerlin, B. S.; Matyjaszewski, K. Prog Polym Sci 2008, 33, 759–785.
17. Cheng, G.; Bolker, A.; Zhang, M.; Krausch, G.; Muller, A. H. E. Macromolecules 2001, 34, 6883–6888.

18. Djalali, R.; Hugenberg, N.; Fischer, K.; Schmidt, M. Macromol Rapid Commun 1999, 20, 444–449.
19. Lanson, D.; Schappacher, M.; Deffieux, A.; Borsali, R. Macromolecules 2006, 39, 7107–7114.
20. Khelfallah, N.; Gunari, N.; Fischer, K.; Gkogkas, G.; Hadjichristidis, N.; Schmidt, M. Macromol Rapid Commun 2005, 26, 1693–1697.
21. Yi, Z.; Liu, X.; Jiao, Q.; Chen, E.; Chen, Y.; Xi, F. J Polym Sci Part A: Polym Chem 2008, 46, 4205–4217.
22. Cheng, Z.; Zhu, X.; Fu, G. D.; Kang, E. T.; Neoh, K. G. Macromolecules 2005, 38, 7187–7192.
23. Xu, X.; Jia, Z.; Sun, R.; Huang, J. J Polym Sci Part A: Polym Chem 2006, 44, 4396–4408.
24. Cao, H.; Lin, W.; Liu, A.; Zhang, J.; Wan, X.; Zhou, Q. Macromol Rapid Commun 2007, 28, 1883–1888.
25. Zamurovic, M.; Christodoulou, S.; Vazaios, A.; Iatrou, E.; Pitsikalis, M.; Hadjichristidis, N. Macromolecules 2007, 40, 5835–5849.
26. Jin, L.; Liu, P.; Hu, J.; Wang, C. Polym Int 2004, 53, 142–148.
27. Otsuka, H.; Nagasaki, Y.; Kataoka, K. Curr Opin Colloid Interface Sci 2001, 6, 3–10.
28. Dunn, S. E.; Brindley, A.; Davis, S. S.; Davies, M. C.; Illum, L. Pharm Res 1994, 11, 1016–1022.
29. Checot, F.; Lecommandoux, S.; Gnanou, Y.; Klok, H.-A. Angew Chem Int Ed 2002, 41, 1339–1343.
30. Rodriguez-Hernandez, J.; Lecommandoux, S. J Am Chem Soc 2005, 127, 2026–2027.
31. Kukula, H.; Schlaad, H.; Antonietti, M.; Forster, S. J Am Chem Soc 2002, 124, 1658–1663.
32. Borner, H. G.; Schlaad, H. Soft Matter 2007, 3, 394–408.
33. Rao, J.; Luo, Z.; Ge, Z.; Liu, H.; Liu, S. Biomacromolecules 2007, 8, 3871–3878.
34. Holowka, E. P.; Pochan, D. J.; Deming, T. J. J Am Chem Soc 2005, 127, 12423–12428.
35. Harada, A.; Nakanishi, K.; Ichimura, S.; Kojima, C.; Kono, K. J Polym Sci Part A: Polym Chem 2009, 47, 1217–1223.
36. Kuo, S.-W.; Lee, H.-F.; Huan, C.-F.; Huang, C.-J.; Chang, F.-C. J Polym Sci Part A: Polym Chem 2008, 46, 3108–3119.
37. Xu, N.; Du, F.-S.; Li, Z.-C. J Polym Sci Part A: Polym Chem 2007, 45, 1889–1898.
38. Lavasanifar, A.; Samuel, J.; Kwon, G. S. Adv Drug Delivery Rev 2002, 54, 169–190.
39. Brown, M. D.; Gray, A. I.; Tetley, L.; Santovena, A.; Rene, J.; Schatzlein, A. G.; Uchegbu, I. F. J Controlled Release 2003, 93, 193–211.
40. Sun, J.; Deng, C.; Chen, X.; Yu, H.; Tian, H.; Sun, J.; Jing, X. Biomacromolecules 2007, 8, 1013–1017.
41. Qiu, S.; Huang, H.; Dai, X.-H.; Zhou, W.; Dong, C.-M. J Polym Sci Part A: Polym Chem 2009, 47, 2009–2023.
42. Tang, D.; Lin, J.; Lin, S.; Zhang, S.; Chen, T.; Tian, X. Macromol Rapid Commun 2004, 25, 1241–1246.
43. Ding, W.; Lin, S.; Lin, J.; Zhang, L. J Phys Chem B 2008, 112, 776–783.
44. Cai, C.; Zhang, L.; Lin, J.; Wang, L. J Phys Chem B 2008, 112, 12666–12673.
45. Cai, C.; Lin, J.; Chen, T.; Wang, X.-S.; Lin, S. Chem Commun 2009, 2709–2711.
46. Lin, J.; Zhang, S.; Chen, T.; Lin, S.; Jin, H. Int J Pharm 2007, 336, 49–57.
47. Lin, J.; Zhu, J.; Chen, T.; Lin, S.; Cai, C.; Zhang, L.; Zhuang, Y.; Wang, X.-S. Biomaterials 2009, 30, 108–117.
48. Wei, L.; Cai, C.; Lin, J.; Chen, T. Biomaterials 2009, 30, 2606–2613.
49. Blout, E.; Karlson, R. J Am Chem Soc 1956, 78, 941–946.
50. Lin, J.; Abe, A.; Furuya, H.; Okamoto, S. Macromolecules 1996, 29, 2584–2589.
51. Koide, A.; Kishimura, A.; Osada, K.; Jang, W.-D.; Yamasaki, Y.; Kataoka, K. J Am Chem Soc 2006, 128, 5988–5989.
52. Knoop, R. J. I.; Habraken, G. J. M.; Gogibus, N.; Steig, S.; Menzel, H.; Koning, C. E.; Heise, A. J Polym Sci Part A: Polym Chem 2008, 46, 3068–3077.
53. Gibson, M. I.; Cameron, N. R. J Polym Sci Part A: Polym Chem 2009, 47, 2882–2891.
54. Kricheldorf, H. R.; Lossow, C. V.; Lomadze, N.; Schwarz, G. J Polym Sci Part A: Polym Chem 2008, 46, 4012–4020.
55. Higashi, N.; Koga, T.; Niwa, M. Adv Mater 2000, 12, 1373–1375.
56. Higashi, N.; Kawahara, J.; Niwa, M. J Colloid Interface Sci 2005, 288, 83–87.
57. Ibarboure, E.; Rodriguez-Hernandez, J.; Paon, E. J Polym Sci Part A: Polym Chem 2006, 44, 4668–4679.
58. Sugimoto, H.; Nakanishi, E.; Yamauchi, F.; Yasumura, T.; Inomata, K. Polymer 2005, 46, 10800–10808.
59. Kricheldorf, H. R. Alpha-Amino Acid-N-Carboxy Anhydrides and Related Heterocycles; Springer-Verlag: Berlin, 1987.
60. Wu, C.; Li, M.; Kwan, S.; Liu, G. Macromolecules 1998, 31, 7553–7554.
61. Chu, B. Laser Light Scattering, 2nd ed.; Academic Press: New York, 1991.
62. Bang, J.; Jain, S.; Li, Z.; Lodge, T. P. Macromolecules 2006, 39, 1199–1208.
63. Antonietti, M.; Forster, S. Adv Mater 2003, 15, 1323–1333.
64. Zhou, Z.; Li, Z.; Ren, Y.; Hillmyer, M. A.; Lodge, T. P. J Am Chem Soc 2003, 125, 10182–10183.
65. Lin, S.; Numasawa, N.; Nose, T.; Lin, J. Macromolecules 2007, 40, 1684–1692.
66. Jenekhe, S. A.; Chen, X. L. Science 1999, 283, 372–375.
67. Lee, M.; Cho, B.-K.; Zin, W.-C. Chem Rev 2001, 101, 3869–3892.